SECM/15/011

Temporary Substructure Forces during Bridge Slide: Impact of Sliding Friction and Substructure Alignment

O. U. Ridvanoglu[1], U. B. Attanayake [1*] and H. M. Aktan[1]

[1]Western Michigan University, Kalamazoo, United States
E-Mail: upul.attanayake@wmich.edu, TP: +1 269 276 32 11

Abstract: Slide-in Bridge Construction (SIBC) is different from the conventional bridge construction because of the activity required to move the bridge to final position following construction. Moving activity requires bridge to be on a temporary support structure, resting on a sliding system such as bearings suitable for sliding, and a system of force actuation for pushing or pulling the bridge. Two SIBC projects were recently completed in Michigan, USA. SIBC being new to the bridge community, substructure forces that are developed during slides are best estimated. Hence, one of the Michigan projects was selected and slide operation was simulated using dynamic explicit finite element analysis techniques. This article presents use of dynamic explicit finite element analysis for evaluating temporary substructure forces during bridge slide. Further the analysis results are used to explain the impact of unequal friction at sliding surfaces and differential alignment of the temporary supports on substructure forces and bridge superstructure movement. Typically, bridge superstructures are slid in place using force-controlled systems. Analysis was performed using force-controlled and displacement-controlled methods. Then, the analysis results are used to explain the benefits of using displacement-controlled methods with force monitoring to slide a bridge rather than employing a force-controlled method.

Keywords: Accelerated Bridge Construction (ABC), Dynamic Explicit Simulation, Finite Element Analysis, Parametric Analysis, Slide-In Bridge Construction

1. Introduction

The Slide-in Bridge Construction (SIBC) is performed by supporting a new superstructure on sliding girders and pulling them, or by installing sliding surfaces to a new superstructure itself and pushing it. Two SIBC projects were completed in Michigan [0, 0]. During both projects, new superstructures were moved by applying forces and monitoring displacements. Displacement was monitored visually by construction personal, and the moving operation was temporarily stopped every time the bridge superstructure was off the alignment by a magnitude specified in the project special provisions. This process caused many challenges to the contractor for maintaining bridge alignment.

In order to demonstrate the impact of using force control and displacement control sliding, differential friction at the sliding surfaces, and differential alignment of the temporary substructure, sliding of the US-131 NB Bridge over 3 Mile Road in Michigan, USA, was simulated. This article presents the simulation model, temporary structure forces developed during slide, challenges with maintaining bridge alignment with differential friction under force or displacement-controlled slide, and recommendation to overcome some of the challenges experienced during SIBC.

2. Sliding friction

Friction at the sliding surface plays an important role in SIBC. Static and kinetic friction coefficients are used to calculate the required pull or push forces to slide a bridge as well as to design temporary and permanent substructure. Identifying and evaluating the parameters that affect static and kinetic friction coefficients and the decay rate from static to kinetic friction is important to properly design a slide system. According to the classical isotropic Coulomb friction model shown in Eq. 1, the friction at a given time can be calculated knowing the static and kinetic friction coefficients as well as the exponential decay rate [0].

$$\mu = \mu_k + (\mu_s - \mu_k)e^{d_c \dot{\gamma}_{eq}} \quad (1)$$

where, μ_k and μ_s are the kinetic and static friction coefficients, d_c is a decay coefficient, and γ_{eq} is the slip rate.

As shown in Figure 1, a typical sliding surface used in SIBC is formed by placing a stainless steel shoe on a set of neoprene bearing pads with Polytetrafluoroethylene (PTFE) layers (PTFE is commonly known as *Teflon*). Hence, the interface between a sliding shoe and PTFE layers form the sliding surface. Friction at PTFE-stainless steel sliding surfaces depends on sliding velocity, normal pressure, PTFE composition, steel sliding surface roughness, surface treatment (lubricants), temperature, and the angle between the surface polishing of steel and sliding direction [0].

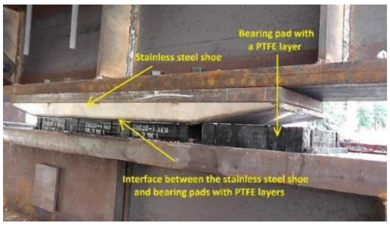

Figure 1: A stainless steel sliding shoe and neoprene bearing pads with PTFE layers

Kinetic friction decreases with an increase in normal pressure and use of lubrication [0]. Published data in many resources was reviewed [0 - 0]. In summary, static and kinetic friction coefficients range from 4% to 15% and from 1% to 6%, respectively. Unfortunately, references do not explicitly document the type of PTFE and the conditions under which the data was recorded. Kinetic friction coefficients given in the jacking plans for Michigan slide projects [0] and SHRP 2 R04 [0] are primarily from the AASHTO LRFD [0] for dimpled lubricated PTFE pads with less than 1 ksi (6895 kPa) normal pressure. Considering the data given in [0 – 0 and 0 - 0], static friction of 10% and a kinetic friction coefficient range of 2% - 5% are selected for the analysis.

3. Simulation of SIBC

3.1 US-131 NB Bridge construction

The US-131 NB over 3 Mile Road SIBC project was considered as a case-study. The new superstructure was built on temporary substructures located outside of the existing alignment of the bridge, but adjacent to the old structure (Figure 2a). Temporary substructure at each abutment location consisted of HP14×73 driven piles, HP14×73 columns, a railing girder, a transition girder, and a sliding girder. Each temporary substructure consisted of 8 vertically driven H-piles and 4 battered H-piles. At alternate pile locations, battered piles were added to provide lateral stiffness to the substructure. At those locations, a short HP14×73 section was welded on top as an extension to provide lateral restraint to the superstructure during construction. Spread box beams of the replacement structure were supported by wooden blocks on the sliding girder (Figure 2b). Neoprene bearing pads with PTFE layers were placed next to each other along the railing girder to form the sliding surface. Two post-tensioning jacks with a maximum stroke of 2 in. (50 mm) and a capacity of 110 ton (978.6 kN) were mounted to pull the superstructure (Figure 2c). Both jacks were powered by a single hydraulic pump. During the pulling operation the pressure was kept equal on both jacks and adjusted manually as needed. Due to limited stroke of the jacks, bridge superstructure was moved by performing a series of discrete pulls instead of pulling the bridge continuously to the final position (Figure 2d).

(a) Temporary substructure for US-131 NB

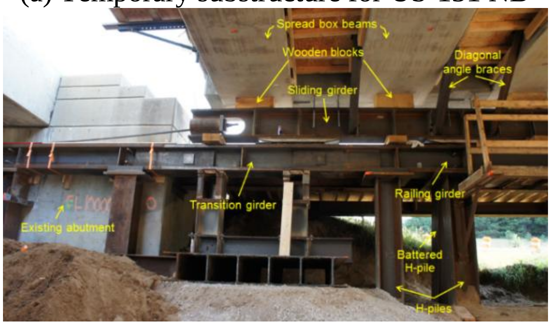

(b) New superstructure on the sliding girder

(c) Sliding girder being pulled

(d) Repositioning a jack after completing a pull

Figure 2: Replacing US-131 NB bridge superstructure using SIBC

The new superstructure geometry on the temporary structure is shown in Figure 3. The railing girder at abutment B was located at a higher elevation than the railing girder at abutment A.

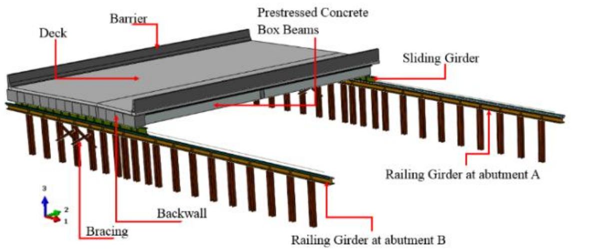

Figure 3: Isometric view of new superstructure on temporary substructure

3.2 Scope of sliding simulation

The scope simulation is shown in Figure 4. The primary objective is to evaluate the impact of interface friction and railing girder alignment on superstructure movement and stresses/stress resultants developed in the temporary structures due to continuous and discrete sliding under displacement and force control methods.

For displacement or force control sliding, railing girders at abutment A and B are positioned at the same alignment or at different alignments (as per the bridge plans, abutment B railing girder was at 0.31 ft (9.4cm) above the railing girder at abutment A). Equal and unequal friction at the sliding surfaces was also considered. With continuous sliding, the superstructure is slid from beginning to end without a pause. Discrete sliding is simulated by pulling the superstructure and allowing it to stop due to frictional forces; a representation of a typical slide.

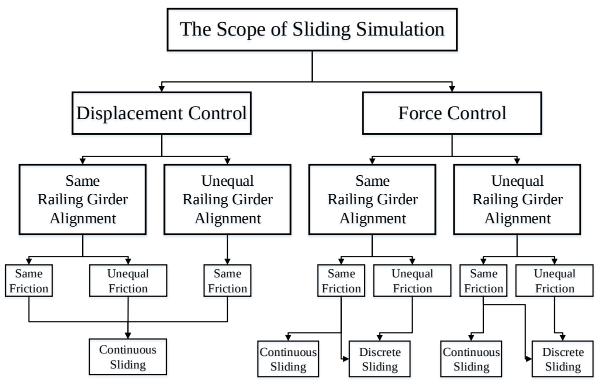

Figure 4: Scope of sliding simulation

3.3 Finite element model (FEM) parameters

3.3.1 Geometry

The US-131 NB bridge geometry and the temporary structure and sliding mechanism details are closely replicated (Figure 3 and Figure 5).

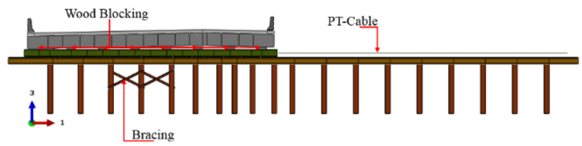

(a) Side view

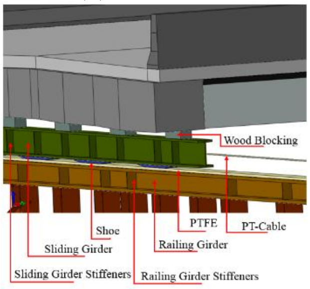

(b) Sliding and railing girder details

Figure 5: Superstructure, temporary structure, and sliding mechanism detail

3.3.2 Normal pressure and friction

As discussed in section 2, static friction of 10% and a kinetic friction coefficient range of 2% - 5% are selected for the analysis. Decay rate depends on static friction, kinetic friction, and sliding velocity. Considering the total length of slide and the slide duration of US-131 over 3 Mile Road project, sliding velocity of 2 in/min (5 cm/min) was calculated. Since the sliding process consisted of a collection of successive discrete sliding events, much higher peak velocities are expected. Further, with experience, it is possible to achieve a peak slide velocity of at least two to three times the velocities that were calculated from the first two SIBC projects in Michigan. Hence, it is reasonable to expect a sliding velocity of 6 in/min (15.2 cm/min) (i.e., 0.1 in/sec) or greater during a discrete event.

As shown in Figure 4, continuous and discrete slide events are simulated. Continuous slide simulation represents a single event during which the bridge is pulled 62.5 ft (19 m) (from start to the end) without a pause. After performing exploratory analyses of sliding events, it is decided to use a sliding velocity of 10 in/sec (25 cm/sec). This decision is made mainly considering the complexity of the analysis model in the presence of a large number of contact surfaces, analysis duration, and space required for storing analysis data during each step of calculation. Using velocities higher than the velocities documented in the field do not affect frictional forces developed at the PTFE – steel interface. This is mainly because the Coulomb friction model is used with user defined static and kinetic friction coefficients and a decay rate. However, using higher velocities may affect the dynamic forces developed in the system when sliding stops. This will be discussed with discrete slide analysis results. For continuous analysis, decay rate is defined to achieve 5% friction when the velocity reaches 10 in/sec (25.4 m/sec), resulting in a decay rate of 0.4105.

Analysis is also performed with unequal friction at two railing girders. In this case, the static friction is maintained at the same, and the kinetic friction of 2% and 5% is defined for the railing girder at abutments A and B, respectively. These values represent an extreme case of unequal friction on sliding girders.

3.2.3 FE Discretization of the model

The railing girder is supported on extended piles or columns, and represent the behaviour of a multi-span continuous beam under moving loads. Because of the girder deflection profile under moving loads, it is expected to have a non-uniform load distribution among the sliding shoes; thus unequal frictional forces between sliding shoes. When unbalanced forces are developed at each sliding girder, there is a possibility for superstructure to yaw.

Since the primary focus is on the interface friction forces, bridge movement, and stress resultants on temporary structures, the bridge superstructure is discretised into a coarse mesh. The members of the temporary substructures, sliding shoes, and the railing girders are discretised into elements with aspect ratios that are suitable for stress calculation.

The contact pair option in Abaqus [0] is used to define the interaction at the interface between the polished stainless steel shoe and the PTFE pads. Multi-point constraint option is used to define the connection between the pulling rods and the sliding girder.

Extended pile and column ends at the ground level are constrained for translations and rotations simulating fixed supports. While one end of the pulling rod is connected to the sliding girder, the other end is constrained for all the degrees of freedoms, except for the translation in direction 1 (i.e., the slide direction shown in Figure 5).

3.2.4 Loads and prescribed displacements

Self-weight of all the components is applied using the *DLOAD command in Abaqus. In order to suppress the dynamics that are not naturally occurring in the system, self-weight is applied as a gradually increasing load using the *AMPLITUDE command. For consistent units, the gravitational acceleration is defined as 386 in/s^2 (9.81 m/s^2).

For displacement control models, a displacement is defined at the free end of the pulling rod. The magnitude of the prescribed displacement is equal to the total slide distance. For force control models, pulling force is defined at the free end of the pulling rod. The total frictional force of 144 kips (640 kN) is calculated based on the nominal stress at each sliding shoe and the static friction coefficient of 10%. However, it is necessary to apply a pulling force that is slightly greater than the estimated total frictional force. Hence, a gradually increasing pulling force with a maximum of 85 kips (378 kN) is applied to each rod.

The force control method is used to simulate a discrete slide event. In this case, the applied force is gradually increased until the sliding structure reaches a predefined velocity. At that time, the force is removed, and the superstructure is allowed to slide until it is stopped due to frictional resistance.

4 Results

4.1 Continuous slide

Continuous sliding simulations were performed under displacement and force control methods. In displacement control, the structure was pulled gradually, starting from a resting position, until the sliding velocity reached 10 in/sec. After that, a constant velocity of 10 in/sec (25.4 cm/sec) was maintained. As a result, both sliding girders slid uniformly along the railing girders, irrespective of the frictional forces developed at the PTFE-steel interface.

Under force control sliding, the structure is expected to slide when the applied force exceeds the resisting force of 72 kips (320 kN). In the analysis described herein, the pulling force was gradually applied to each sliding rail using a ramp function. Hence, the force was gradually increased to 85 kips (378 kN) and maintained at that level until bridge slid 62.5 ft (19 m).

4.1.1 Frictional forces

Frictional forces developed under the displacement control sliding method are presented in Figure 6a. As soon as the sliding initiates, there is a sudden increase in the frictional force. As the velocity increases, the frictional force decreases due to a reduction in the coefficient of friction as per the defined decay rate. With a constant sliding velocity, the frictional force becomes a constant.

Frictional forces developed during force control sliding are presented in Figure 6b. The frictional force is linearly proportional to the applied force until the applied force equals the static frictional force. As the velocity increases, the frictional force decreases in proportion to the defined decay rate. Once the friction reaches kinetic friction, frictional force remains constant during the rest of the move.

The static friction coefficient at each sliding surface is specified as 10%. The vertical force acting on each temporary structure is 720 kips (3200 kN). Hence, the expected total frictional force on each temporary structure at the onset of sliding, and in the direction of sliding, is 72 kips (320 kN) (i.e., 0.1×720). At the onset of sliding under displacement, the maximum total frictional force observed on each temporary structure in the direction of sliding is 65 kips (289 kN). Similarly, the maximum total frictional force observed on each temporary structure under force control is 69 kips (307 kN). The maximum value is an instantaneous value and, in both cases, the observed forces are more than 90% of the expected value, and within the acceptable limits for numerical simulations. The difference is due to a numerical error with force being calculated at each time increment. The time increment used in the calculations is less than 10^{-5} seconds.

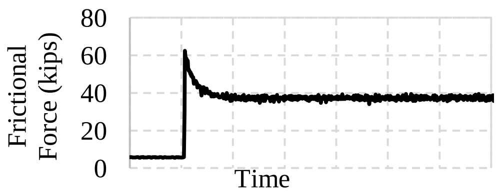

(1 kip = 4.4482 kN)
(a) Displacement control sliding

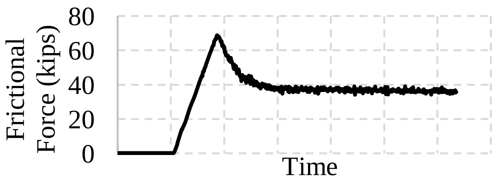

(1 kip = 4.4482 kN)
(b) Force control sliding

Figure 6: Frictional force at Steel-PTFE interface

As shown in Figure 6, when the velocity is equal or greater than 10 in/sec, the frictional forces developed at each rail are 36 kips (160 kN), same as the expected kinetic friction (i.e., 0.05 ×720 kips). The expected value is calculated through numerical simulations because the kinetic friction remains at a constant value over a time during steady state sliding.

In order to account for the friction variation between sliding surfaces, the railing girder at abutments A and B are assigned kinematic friction coefficients of 2% and 5%, respectively. Both temporary structures are assigned the same static friction coefficient of 10%; hence, it is expected to have the same maximum frictional force acting on both temporary structures. Forces acting on each structure at the onset of sliding are slightly different. As the velocity increases and reaches steady state sliding velocity of 10 in/sec, the forces are decreased to 15 kips (67 kN) and 36 kips (160 kN) for temporary structures at abutments A and B, respectively. Even with unequal friction, under displacement control, the sliding progresses in alignment without any drift to the transverse direction. Unequal friction simulations under force control was not performed for continuous slide. Under force control, even a small difference in friction will drift the structure to the transverse direction. For a continuous slide, since the sliding distance is greater, performing unequal friction simulation without transverse restraint under force control method will move the sliding girder off the alignment making the system unstable. Hence, only discrete slide was simulated under force control with unequal friction and the results are presented in the following section 4.2.

4.1.2 Forces on temporary structure

Forces generated at the sliding surfaces are the horizontal forces that are transmitted to the temporary structure. The normal forces at the sliding surface and the temporary structure self-weight represent the vertical reactions at the temporary structure supports. In design, the vertical loads are calculated from the dead loads. The horizontal load is calculated from static friction and the normal force acting on the sliding surface. Sliding can also generate dynamic loads.

The analysis results are useful to understand the structural response and the nature of forces that are developed during a bridge slide. Figure 7 shows the variation of superstructure velocity and reaction forces developed in the temporary structure under displacement and force control sliding. The horizontal reaction expected at the temporary structure under static friction is 72 kips (320 kN). Due to the acceleration introduced into the system at the onset of sliding under displacement control, the horizontal forces greater than 100 kips (444.82 kN) are developed. As per the displacement control analysis parameters used in this analysis, an impact factor of 1.53 (i.e., 110 kips/72 kips) is calculated. The application of well controlled slower displacement rates (i.e., velocities) at the beginning of a slide can reduce these dynamic forces.

In displacement control sliding simulation, the rate of displacement (i.e., velocity) is increased from zero to 0.833 ft/s (0.26 m/sec) (i.e., 10 in/sec) within a short duration, and it is maintained at a constant rate afterwards (Figure 7a). The change in the rate of displacement resulted in an acceleration that amplified the inertia forces acting on the superstructure. However, under force control sliding simulation, initial motion of the bridge superstructure is slow, and the rate of change of velocity is quadratic until achieving a linear profile (Figure 7b). Because of the small acceleration at the beginning of the motion, dynamic effects are not significant. Sliding structure dynamics affected the vertical reactions, too. However, the amplifications are less than 2% and 1% in displacement and force control sliding, respectively.

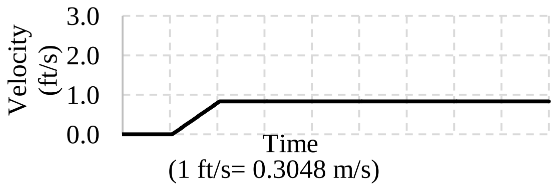

(a) Displacement control sliding

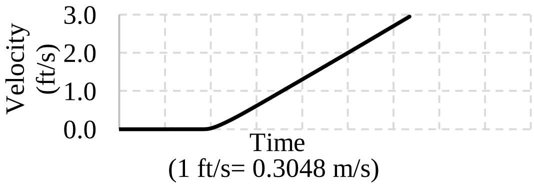

(b) Force control sliding

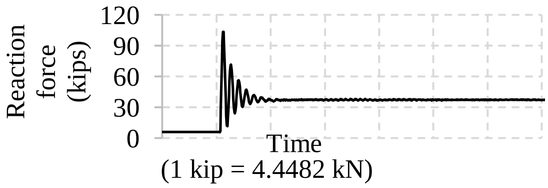

(c) Displacement Control sliding

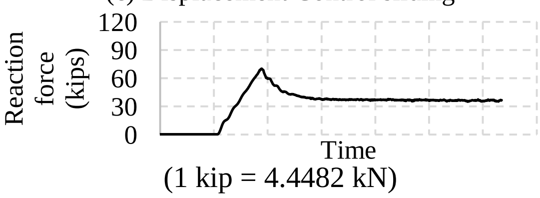

(d) Force Control sliding

Figure 7: Variation of velocity and temporary structure's horizontal reaction in the sliding direction for displacement and force control sliding

4.1.3 Unequal railing girder alignment

Slide simulation was performed with an unequal railing girder alignment. During this simulation, a uniform friction on both railing girders was maintained. Simulation was performed using displacement and force control methods. The alignment difference between abutments was 0.31 ft (9.45 cm) which is equivalent to a 0.4% grade of the superstructure. Displacement control continuous slide resulted in a 0.75 in (1.9 cm) transverse drift towards abutment A. This is less than the 1 in. (2.54 cm) tolerance specified in project special provisions. Since same friction was maintained on both railing girders, frictional forces acting on each temporary structure remained the same. Under force control simulation no significant transverse movement was observed.

4.2 Discrete slide

Pulling or pushing of a bridge superstructure is not a continuous operation. The superstructure is pulled or pushed up to a certain distance depending on the stroke capacity of the jacks. The impact of this pulling or pushing process on the sliding process, as well as on the temporary structure, was of an interest.

Under force control sliding, the structure is expected to start sliding as soon as the pulling force overcomes the resisting force of 72 kips (320 kN). The pulling force was gradually increased to 85 kips (378 kN) and maintained at that level until the velocity reached to 10 in/s. At that time, the force was removed and allowed the structure to slide for a while under inertia and frictional forces. The following four cases were considered for discrete sliding:

Case I:

- Both railing girders are at the same elevation.
- Equal friction occurs on both girders (10% static and 5% kinetic).

Case II:

- Unequal railing girder alignment (railing girder at abutment B is raised 0.31 ft above the railing girder at abutment A).
- Equal friction occurs on both girders (10% static and 5% kinetic).

Case III:

- Both railing girders are at the same elevation.

- Unequal kinetic friction occurs on railing girders (10% static on both, and 2% and 5% kinetic friction on railing girder at abutment A and B respectively).

Case IV:

- Unequal railing girder alignment (railing girder at abutment B is raised 0.31 ft (9.4 cm) above the railing girder at abutment A).
- Unequal kinetic friction occurs on railing girders (10% static on both, and 2% and 5% kinetic friction on railing girder at abutments A and B respectively).

Out of the four simulation cases listed above, only Case I and Case III were included for further analysis. According to preliminary analysis, unequal railing girder alignment does not have significant effects on the simulation results. This is mainly due to the limited slide distance under discrete sliding. The difference between Case I and III is the friction coefficients of railing girders. Case I incorporates equal friction while Case III includes unequal friction on girders.

4.2.1 Sliding frictional forces

Initially, the frictional forces follow the same trend and pattern that was observed during continuous sliding under force control. As shown in Figure 8a, frictional force was gradually increased up to 69 kips (307 kN). Once the motion started, velocity was increased, and frictional force was reduced to 38 kips (169 kN), following the decay rate defined in the friction model. After the pulling force was removed, the velocity was gradually reduced and the frictional forces started to increase in proportion to the decay rate defined in the friction model. By the time the structure sliding seized, frictional forces reached the maximum, the static value. At this moment, dynamic forces were developed in the structure. Similar behaviour was observed when kinetic friction of 2% and 5% were assigned to abutment A and B (Figure 8b). The maximum dynamic frictional force of 32 (142 kN) kips was observed.

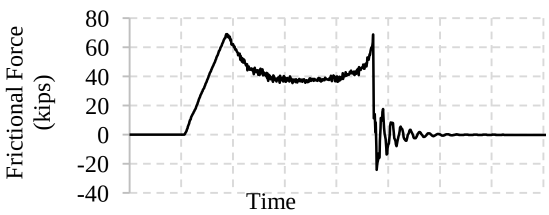

(1 kip = 4.4482 kN)
(a) Case I

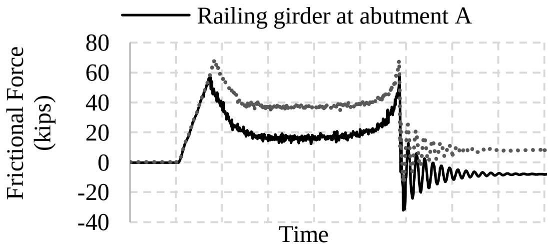

(1 kip = 4.4482 kN)
(b) Case III

Figure 8: Frictional force developed under discrete sliding

Due to unequal friction, bridge superstructure drifted to transverse direction and engaged with the restraint provided in the model. One inch (25.4 mm) tolerance was maintained between sliding girder and the restraint. As soon as the structure engaged with the restraint, it bounced back and drifted again to engage with the transverse restraint. This movement was repeated and the superstructure started sliding against the restraint provided in the system. Analysis results demonstrate the need for providing transverse restraint even if the railing girders are at the same alignment.

4.2.2 Forces on temporary structure

Figure 9 shows the temporary structure's horizontal reactions, in the direction of sliding, with respect to time. Analysis cases are (a) equal railing girder alignment with equal friction and (b) equal railing girder alignment with unequal friction. As shown in Figure 9, once the superstructure sliding was seized, dynamic forces were developed at the supports. The maximum amplitude of the dynamic force was about 72 kips (267 kN). The frictional dynamic force amplitude at the sliding surface ranged between 24 kips (107 kN) and 32 kips (142 kN) (Figure 8). However, due to the inertia forces developed in the substructure, horizontal reactions at the temporary structure supports were amplified. Yet, the damping characteristics of the structural system was adequate to control the response.

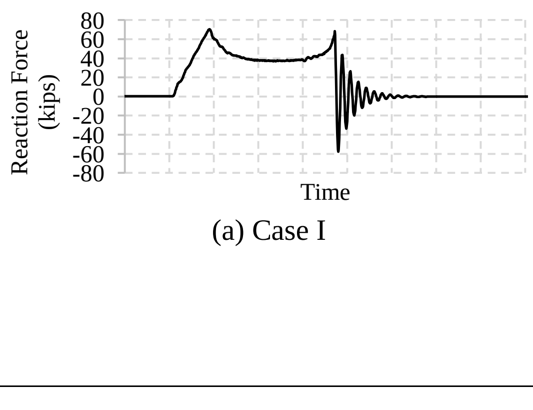

(a) Case I

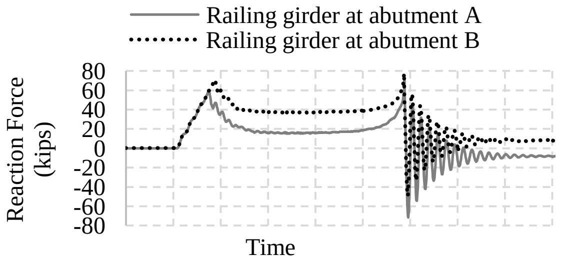

(b) Case III

Figure 9: Temporary structure reactions in the sliding direction

4.2.3 Unequal railing girder alignment

Unequal railing girder alignment of 0.31 ft (9.4 cm) did not generate a noticeable drift. One reason for this can be the limited sliding distance of about 9 ft during this discrete event. Analysis results of unequal railing girder alignment models closely represented the observations discussed in the previous section.

5 Summary, Conclusion and Recommendations

The US-131 over 3 mile (1.6 km) Road Bridge slide-in processes was simulated. The primary objective was to evaluate the impact of interface friction and railing girder alignment on superstructure movement and stresses or stress resultants developed in the temporary structures due to continuous and discrete sliding under displacement and force control methods.

The following conclusions are derived based on the analysis results presented in this article:

1. Dynamic explicit analysis is a versatile tool to simulate bridge slide operations and to evaluate the impact of parameters that affect the sliding process.
2. As a result of unequal friction, the superstructure drifts in the direction transverse to the direction of sliding. Hence, providing a lateral restraint is important to keep the bridge aligned with the slide direction, irrespective of the railing girder alignment differences.
3. Unequal railing girder alignment does not generate a significant drift in continuous sliding. Under displacement control, the superstructure drift under 0.4% grade was less than 1.0 in. (2.54 cm), and within the movement tolerances specified for the project. Drifting is not observed during discrete sliding. Hence, unequal friction has a greater influence than the railing girder alignment on the transverse drift of the superstructure.
4. During discrete sliding, considerably large fluctuations in horizontal reactions, in the direction of slide, were documented at the temporary structure supports. This is a result of the inertia forces developed in the system due to substructure self-weight. Still these dynamic forces are smaller than the static frictional forces. Further, the damping characteristics of the structural system was adequate to control the response. Hence, use of the horizontal forces due to static friction is adequate for design of temporary substructures. However, the structural system dynamic characteristics needs to be studied to evaluate potential for resonance.
5. Implementation of the displacement control sliding method allows sliding the superstructure without transverse drift, irrespective of the difference in friction of the sliding surfaces. To define accurate and controlled displacement and force targets during the move operation, a servo controller is required. The inclusion of the servo controller requires the use of electronics and most likely a field computer. The advantage of using a servo controller is the ability to establish force, displacement, or combined targets for the movement of the piston. To prevent uncontrolled force built-up, the servo system can be programmed with force limits so that in unforeseen situations, such as the move being restrained, the movement will stop when force limits are reached.

Acknowledgement

This project is funded by the Michigan Department of Transportation. The authors would like to acknowledge the support extended by Mr. David Juntunen, Mr. Corey Rogers, and the research advisory panel members for successful completion of the project. Support and efforts of Mr. Abdul Mohammed is greatly appreciated.

References

[1]. Aktan, H., Attanayake, U., and Mohammed, A. W., "Michigan Department of Transportation Bridge Slide Showcase", the Michigan Department of Transportation, Lansing, MI, USA, 2015.

[2]. Aktan, H., Attanayake, U., "Research on Evaluation and Standardization of Accelerated Bridge Construction Techniques", the Michigan Department of Transportation, Lansing, MI, USA, 2015.

[3]. Oden, J. T., Martins, J. A. C., “Models and Computational Methods for Dynamic Friction Phenomena”, J. of Computer Methods in Applied Mechanics and Engineering, Elsevier, 52(1-3), 527–634, 1985.

[4]. Hwang, J. S., Chang, K. C., and Lee, G. C., "Quasi-Static and Dynamic Sliding Characteristics of Teflon-Stainless Steel Interfaces", Journal of Structural Engineering, 2747-2762, 1990.

[5]. AASHTO LRFD Bridge Design Specifications, Customary U.S. Units, 7th ed., American Association of State Highway and Transportation Officials, Washington, DC, 2014.

[6]. Bondonet, G., Filitrault, A., "Frictional Response of PTFE Sliding Bearings at High Frequencies", Journal Of Bridge Engineering, 2:139-148, 1997.

[7]. Constantinou, M., “Properties of Sliding Bearings: Theory and Experiments”, CISM International Centre for Mechanical Sciences, 97-109, 1994.

[8]. Blau, P. J., Friction Science and Technology from Concepty to Applications, 2nd ed., CRC Press, Boca Raton, 2009.

[9]. Dupond, R., Teflon® PTFE Properties Handbook, Wilmington, DE.

[10].MDOT.. M-50 Bridge Jacking Plans-Mammoet Company, Michigan Department of Transportation (MDOT), Lowell, MI, 2014

[11] SHRP 2 R04, ABC Standard Concepts: The Lateral Slide Addendum Report, Transportation Research Board of the National Academies, Washington, D.C, 2015

[12].Dassault Systemes.,Abaqus 6.14 Analysis User Manual, Providence, RI, USA, (2014)